

NACA RM L54B23



RESEARCH MEMORANDUM

PRESSURE RECOVERY AND DRAG CHARACTERISTICS OF A FORWARD
LOCATED CIRCULAR SCOOP INLET AS DETERMINED FROM
FLIGHT TESTS FOR MACH NUMBERS FROM 0.8 TO 1.6

By Charles F. Merlet

Langley Aeronautical Laboratory
Langley Field, Va.

~~CLASSIFIED~~
UNCLASSIFIED

To _____

By authority of NACA Res abs
4 RN-125 Date effective
AmT 3-21-58 Feb. 26, 1958

CLASSIFIED DOCUMENT

This material contains information affecting the National Defense of the United States within the meaning of the espionage laws, Title 18, U.S.C., Secs. 793 and 794, the transmission or revelation of which in any manner to an unauthorized person is prohibited by law.

NATIONAL ADVISORY COMMITTEE
FOR AERONAUTICS

WASHINGTON

April 8, 1954

LIBRARY COPY

APR 8 1954

LANGLEY AERONAUTICAL LABORATORY
LIBRARY, NACA
LANGLEY FIELD, VIRGINIA

NATIONAL ADVISORY COMMITTEE FOR AERONAUTICS

RESEARCH MEMORANDUM

PRESSURE RECOVERY AND DRAG CHARACTERISTICS OF A FORWARD
LOCATED CIRCULAR SCOOP INLET AS DETERMINED FROM
FLIGHT TESTS FOR MACH NUMBERS FROM 0.8 TO 1.6

By Charles F. Merlet

SUMMARY

A circular scoop inlet located well forward on a parabolic body of revolution has been flight-tested over a Mach number range from 0.8 to 1.6 at Reynolds number range from 3×10^6 to 9×10^6 , respectively, based on maximum body diameter, and over a range of mass-flow ratios from 0.3 to 1.1. The inlet, installed so that it caused no increase in the frontal area of the configuration, had an area equal to 8 percent of the body frontal area. Test results show that, at maximum mass-flow ratio, the installation of the inlet caused only small differences in drag as compared with the drag of the body alone. The drag increase due to spillage was equal to the theoretically calculated scoop incremental drag at supersonic speeds.

The inlet total-pressure recovery decreased from a value of 1.0 at subsonic speeds to a minimum value of 0.95 at a Mach number of 1.6, the latter value being about 6 percent higher than free-stream normal-shock recovery. Up to a Mach number of 1.4, the inlet total-pressure recovery was approximately constant at all mass-flow ratios, whereas, at a Mach number of 1.6, it decreased slightly with increasing flow rates.

INTRODUCTION

The total-pressure recovery of an air inlet and the effect of its installation on the drag of the configuration are two important considerations involved in the selection of particular inlet configuration. A scoop-inlet configuration, designed with these considerations in mind, has been flight-tested by the Pilotless Aircraft Research Division of the Langley Aeronautical Laboratory. The configuration tested was obtained by locating a circular scoop well forward on a parabolic body of revolution. The forward location was used for two reasons: (1) it allowed

installation of the inlet without increasing the maximum frontal area so as to minimize the effect of the inlet installation on drag and (2) high recoveries would be expected because of the supersonic compression obtained through the attached oblique shock at the tip of the body at supersonic speeds. The circular cross section was selected as an inlet shape that was structurally strong around which the boundary layer could be passed easily, particularly when the inlet is mounted on a circular fuselage.

Prior to flight-testing, extensive supplementary ground calibration tests of the model were made. As tested originally, the pointed nose of the body was drooped toward the inlet to reduce the amount of turning required of the air entering the inlet. The results of these tests employing the drooped nose, presented in reference 1, showed that the high recoveries attained at 0° and 7° angle of attack, both at the inlet and after diffusion, were decreased appreciably at -7° angle of attack. Therefore, the nose of the flight model was made axially symmetric.

The flight test was conducted with a rocket-propelled model in free flight at an angle of attack of 0° . The results of this test are presented herein in the form of external drag coefficients and total-pressure recoveries for a range of mass flow-ratios from Mach numbers of 0.8 to 1.6 and Reynolds numbers from 3×10^6 to 10×10^6 , respectively. The drag of the parabolic body to which the scoop was added is also included for comparison.

SYMBOLS

A	area, sq in.
A_f	frontal area (0.545 sq ft)
D_T	total drag, lb
C_{D_T}	total drag coefficient, $\frac{D_T}{\frac{1}{2}\rho_o V_o^2 A_f}$
$C_{D_{int.}}$	internal drag coefficient, $\frac{m(V_o - V_e) - (P_e - P_o)A_e}{\frac{1}{2}\rho_o V_o^2 A_f}$
C_{D_x}	external drag coefficient, $C_{D_T} - C_{D_{int.}}$

C_{D_s}	scoop incremental drag coefficient, $\frac{m(V_i - V_o) + A_i(p_i - p_o)}{\frac{1}{2}\rho_o V_o^2 A_f}$
C_{D_B}	base drag of nonducted body, $\frac{-(p_B - p_o)A_B}{\frac{1}{2}\rho_o V_o^2 A_f}$
H/H_o	total-pressure recovery (weighted on mass flow) at inlet-minimum-area station
L	total model length, ft
M	Mach number
m	mass flow through the duct, slugs/sec
m/m_o	ratio of mass flowing through duct to mass flow through a free-stream tube of area equal to inlet area at leading edge of lip (6.29 sq in.)
p	static pressure, psia
R	Reynolds number, based on maximum body diameter of 10 inches
V	velocity, ft/sec
X	axial distance from nose of model, ft
ρ	density, slug/ft ³

Subscripts:

o	free stream
i	inlet
e	exit
b	base of nonducted model

MODELS, INSTRUMENTATION, AND TESTS

Models

Photographs and sketches of the models are presented in figures 1 and 2, respectively. The scoop inlet model, similar to that of reference 1, was formed by adding the circular underslung scoop to the basic body. The body profile is formed by two parabolic arcs, each having its vertex at the maximum diameter. The body contours are given in table I. Both models were stabilized by four 60° half-delta fins having an NACA 65A004 airfoil sections and a total exposed area of 3.7 square feet; the configuration is the same as that used on the models of reference 2. The bodies of both models were made of wood. The inlet and ducting of the scoop model were made of aluminum.

Inlet and diffuser detail are shown in figure 3. The inlet area at the leading edge of the lips was 8 percent of the maximum body frontal area. Just downstream of the inlet, the duct was contracted to an area 92 percent of the inlet area. This inlet minimum area was maintained for about 1.5 inches. Two rotating shutters driven by an electric motor were installed to vary the rate of air flow during the flight. The rate of air flow was varied at a frequency of about 1 cycle per second. Analysis of the dynamic response characteristics of the instrumentation showed that this frequency introduced negligible errors in the measurements.

Instrumentation

The basic body model was equipped with a four-channel telemeter. Two longitudinal accelerometers were used: one with a wide range to measure total drag at supersonic speeds and one with a smaller range to obtain more accurate subsonic and transonic total drag data. Pitot stagnation pressure was measured with a tube installed in the tip of the nose of the model. The base pressure was measured by a tube located in the base cavity near the model center line about 10.5 inches forward of the rearward end of the model (fig. 2).

The scoop-inlet model had an eight-channel telemeter. Again, two accelerometers were used to measure total drag, and a pitot stagnation pressure tube was installed in the nose of the model. Three total-pressure tubes were installed along a vertical diameter at the end of inlet-minimum-area section. The tubes were located about 0.06, 0.21, and 0.97 diameters down from the inner duct wall. Two static pressure orifices, in the same plane as the total-pressure tubes but angularly displaced about 20° from the vertical diameter, were manifolded to obtain the static pressure. Duct exit static pressure was obtained with four inner wall orifices equally spaced circumferentially 1 inch upstream from

the end of the model and manifolded together. All pressure and accelerometer data (for both models) were transmitted to ground receiving stations where continuous time histories were recorded on film.

Tests

The flight-test procedure was the same for both models. The model was launched at an elevation angle of 60° and accelerated to maximum speed by a single Deacon rocket motor. After burnout of the rocket motor, drag separation of the booster from the model occurred. All data were obtained in the ensuing period of coasting flight, during which the model decelerated to subsonic speeds along a nearly zero-lift trajectory.

Velocity was determined from CW Doppler radar measurements corrected for winds aloft and flight-path curvature. Ambient air conditions were determined from radiosonde observations. The model flight path was computed from measurements made by an NACA modified SCR 584 tracking radar. The Reynolds number of the tests, based on the 10-inch maximum body diameter, is shown in figure 4 as a function of Mach number. The angle of attack was approximately zero. All tests were conducted at the Langley Pilotless Aircraft Research Station at Wallops Island, Va.

METHOD OF ANALYSIS

The external drag is defined herein as the sum of the dragwise components of the aerodynamic pressure and viscous forces acting on the external surfaces of the model plus the scoop incremental drag, as defined in reference 3. Scoop incremental drag is the algebraic sum of the pressure drag on the entering stream tube and the pressure and viscous drag on that portion of the body wetted by the entering flow. The external drag was determined by subtracting the internal drag from the total drag of the model. Details of the methods of determining these quantities are presented and discussed in reference 2. Because the annular base area at rear of the ducted model is so small, the base drag was assumed to be negligible.

Mass-flow ratio and total-pressure recovery (weighted on mass flow) were computed by numerical integration from pressure measurements made at the inlet-minimum-area station. Because the data of reference 1 showed the total-pressure distribution at this station to be nearly uniform at all flow rates at $M = 1.42$, it is felt that the three total-pressure tubes used in the flight model adequately defined the total pressure at the inlet-minimum-area station. The validity of this assumption is indicated by the comparison of the measured and theoretically calculated values of maximum mass-flow ratio presented in figure 5 as a function of

Mach number. The theoretical values were calculated from one-dimensional theory by assuming that, at the inlet-minimum-area station, the Mach number was 1.0 and the only loss in total pressure resulted from shocks located at the tip of the nose and ahead of the inlet.

Because of the relatively high rate of rotation of the shutters, the measured data contained transient terms at intermediate flow rates as a result of the time rate of change of velocity within the duct. (At maximum and minimum flow rates, the time rate of change of velocity was zero and there were no transient terms.) The maximum values of these transient terms were in all cases less than the estimated accuracy of the data presented below. The data were corrected for these transient terms by the method discussed in reference 2. The data presented herein are representative of steady-state values at all flow rates. The maximum inaccuracies in the data are estimated to be within the following limits:

H/H_0	± 0.01
m/m_0 for $m/m_0 \geq 0.7$	± 0.02
m/m_0 for $m/m_0 = 0.4$	± 0.05
C_{D_x} at $M = 1.4$	± 0.01
C_{D_x} at $M = 0.9$	± 0.02
M	± 0.01

RESULTS AND DISCUSSION

The total and base drag coefficients for the basic body are presented in figure 6 as a function of Mach number. The variation of external drag coefficients of the scoop inlet model with Mach number for several flow rates is presented in figure 7. The subsonic drag coefficient of the scoop inlet model was found to be constant at constant flow rates. At $M > 1.05$, the drag coefficient decreased somewhat with increasing Mach number.

In figure 8, the total-minus-base drag coefficient of the basic body is compared with the external drag of the scoop inlet model at maximum flow rate (shown in fig. 5). The installation of this inlet resulted in only small differences in drag throughout the Mach number range. The data of reference 4, presented for tests up to $M = 1.1$ of a forward-located underslung scoop having a larger inlet of different geometry, showed no drag increment due to the installation of the inlet. These data indicate that, with proper design, the forward location of a scoop can be utilized with small drag penalties at maximum flow rates.

A suggested method of applying the "transonic area rule" concept of reference 5 to an inlet configuration proposes the equivalent area distribution of the inlet configuration be determined by subtracting the maximum entering free-stream tube at $M = 1.0$ from the geometric cross-sectional area distribution of the configuration back of the inlet. A comparison of the area distribution of the scoop-inlet model determined in this manner with the cross-sectional area distribution of the basic body is shown in figure 9 (exclusive of fins, which were identical for both models). The equivalent area distribution of the inlet model differs only slightly from the basic body area distribution. Since the transonic drag rise of the two models differed only slightly (fig. 8), the equivalent area distribution presented for the inlet configuration appears reasonable.

The external drag coefficient increased with decreasing mass-flow ratio as shown in figure 10 for several Mach numbers. Also shown are curves of the external drag coefficient minus the scoop incremental drag coefficient (ref. 3) for the three supersonic Mach numbers. These curves of $C_{D_x} - C_{D_s}$ represent the sum of the pressure and viscous drag forces acting on all the external surfaces of the model, including the surface wetted by the entering flow, and are essentially independent of mass-flow ratio. Thus, it appears that, if any lip suction forces were obtained at reduced flow rates, they were canceled by the increase in pressure drag on the body, most probably on the surface wetted by the entering flow.

Figure 11 presents total-pressure recovery at the inlet minimum area station as a function of Mach number for several flow rates. At $M < 1.1$, the total-pressure recovery was nearly 1.0 for a $\frac{m}{m_0} = 0.8$. As Mach number increased above 1.1, the total-pressure recovery decreased gradually but always exceeded free-stream normal-shock recovery. For example, at $M = 1.6$, the minimum recovery was 0.95, about 6 percent greater than free-stream normal-shock recovery. The high inlet recovery is due to the external supersonic compression furnished by the shock at the tip of the nose. Estimated inlet total-pressure recovery, calculated by assuming an oblique shock at the nose of the model and a normal shock ahead of the inlet, agreed with measured values within the accuracy of the data.

Up to a Mach number of 1.4, the inlet total-pressure recovery was nearly independent of mass-flow ratio for the flow rates tested. (See fig. 12.) At a Mach number of 1.6, the inlet total-pressure recovery decreased slightly with increasing mass-flow ratio. The inlet total-pressure recovery of the present tests agreed, within the accuracy of the data, with that presented in reference 1. (The data from ref. 1 are presented for $\alpha = 7^\circ$, because the nose of the body was drooped about 7° from the horizontal.) Reference 1 also presents data on the subsonic diffuser characteristics of this configuration.

CONCLUSIONS

A flight test has been conducted on a circular scoop inlet located well forward on a parabolic body of revolution. The inlet, installed so that it did not increase the frontal area of the configuration, had an area that was 8 percent of the body frontal area. The results of the test, presented for a range of Mach numbers from 0.8 to 1.6 and a range of mass-flow ratios from 0.3 to 1.1, indicate the following conclusions:

1. At all Mach numbers tested and for maximum mass-flow ratio, the installation of the inlet resulted in only small differences in drag as compared with the drag of the body alone.

2. The sum of pressure- and viscous-drag forces on the external surfaces of the inlet model were nearly independent of mass-flow ratio at any particular supersonic Mach number.

3. The total-pressure recovery measured at the inlet had a minimum value of 0.95 at $M = 1.6$, approximately 6 percent greater than free-stream normal-shock recovery. The total-pressure recovery increased as Mach number decreased and reached a maximum recovery of 1.0 at subsonic speeds.

4. Up to a Mach number of 1.4, the inlet total-pressure recovery was nearly independent of mass-flow ratio, whereas, at $M = 1.6$, it decreased slightly as mass-flow ratio increased.

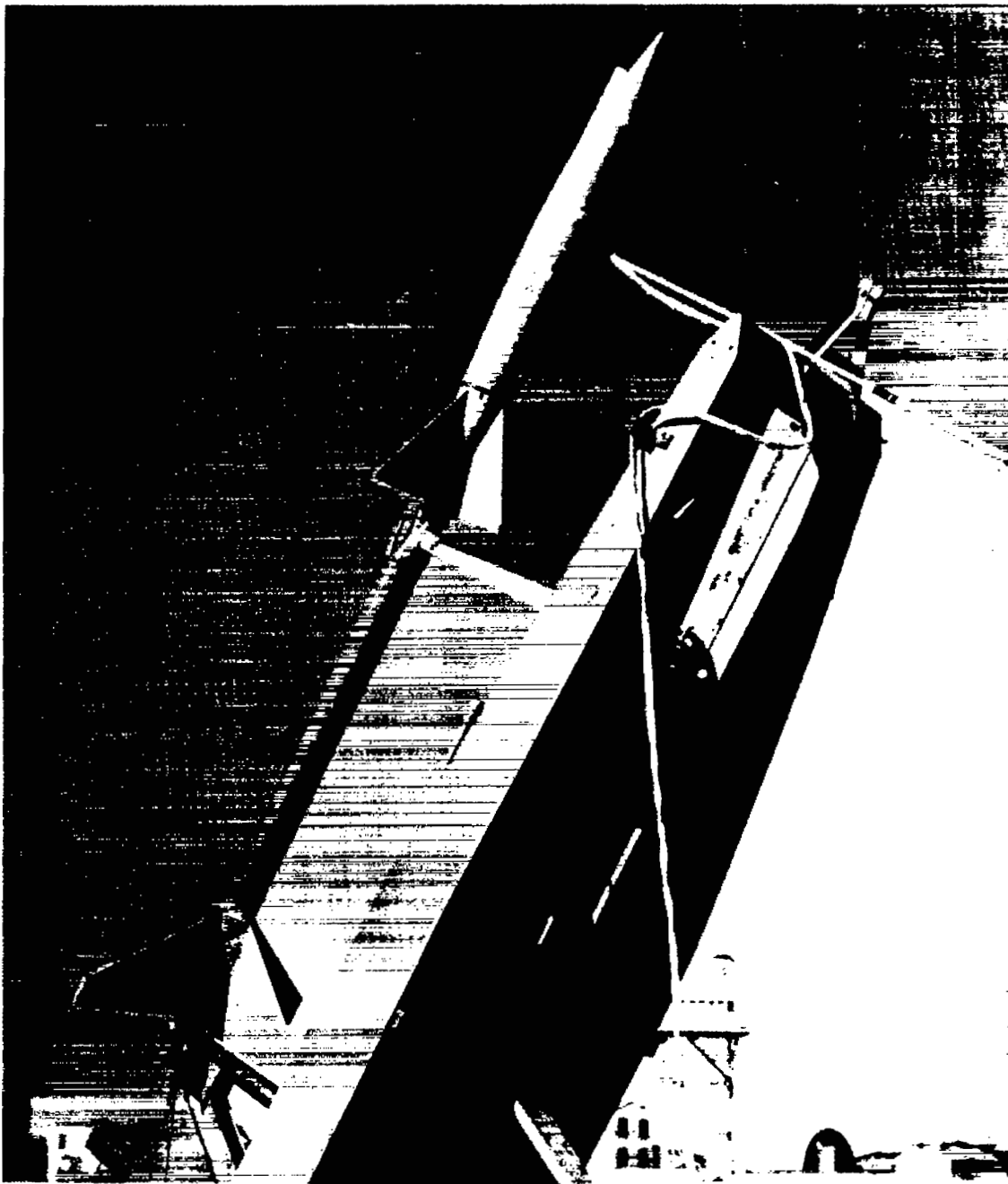
Langley Aeronautical Laboratory,
National Advisory Committee for Aeronautics,
Langley Field, Va., February 9, 1954.

REFERENCES

1. Merlet, Charles F., and Carter, Howard S.: Total-Pressure Recovery of a Circular Underslung Inlet With Three Different Nose Shapes at a Mach Number of 1.42. NACA RM L51KO5, 1952.
2. Sears, Richard I., and Merlet, C. F.: Flight Determination of the Drag and Pressure Recovery of an NACA 1-40-250 Nose Inlet at Mach Numbers From 0.9 to 1.8. NACA RM L50L18, 1951.
3. Klein, Harold: The Calculation of the Scoop Drag for a General Configuration in a Supersonic Stream. Rep. No. SM-13744, Douglas Aircraft Co., Inc., Apr. 12, 1950.
4. Pierpont, P. Kenneth, and Braden, John A.: Investigation at Transonic Speeds of a Forward-Located Underslung Air Inlet On a Body of Revolution. NACA RM L52K17, 1953.
5. Whitcomb, Richard T.: A Study of the Zero-Lift Drag-Rise Characteristics of Wing-Body Combinations Near the Speed of Sound. NACA RM L52H08, 1952.

TABLE I.- COORDINATES FOR PARABOLIC BODY

Station, in.	Radius, in.
0	0
4.00	1.06
8.00	2.00
12.00	2.80
16.00	3.48
20.00	4.06
24.00	4.47
28.00	4.76
32.00	4.95
36.00	5.00
40.00	4.99
44.00	4.93
48.00	4.85
52.00	4.74
56.00	4.59
60.00	4.42
64.00	4.21
68.00	3.97
72.00	3.70
76.00	3.41
80.00	3.07
83.50	2.75
85.00	2.75



(b) Scoop-inlet model on launcher.

L-72601

Figure 1.- Concluded.

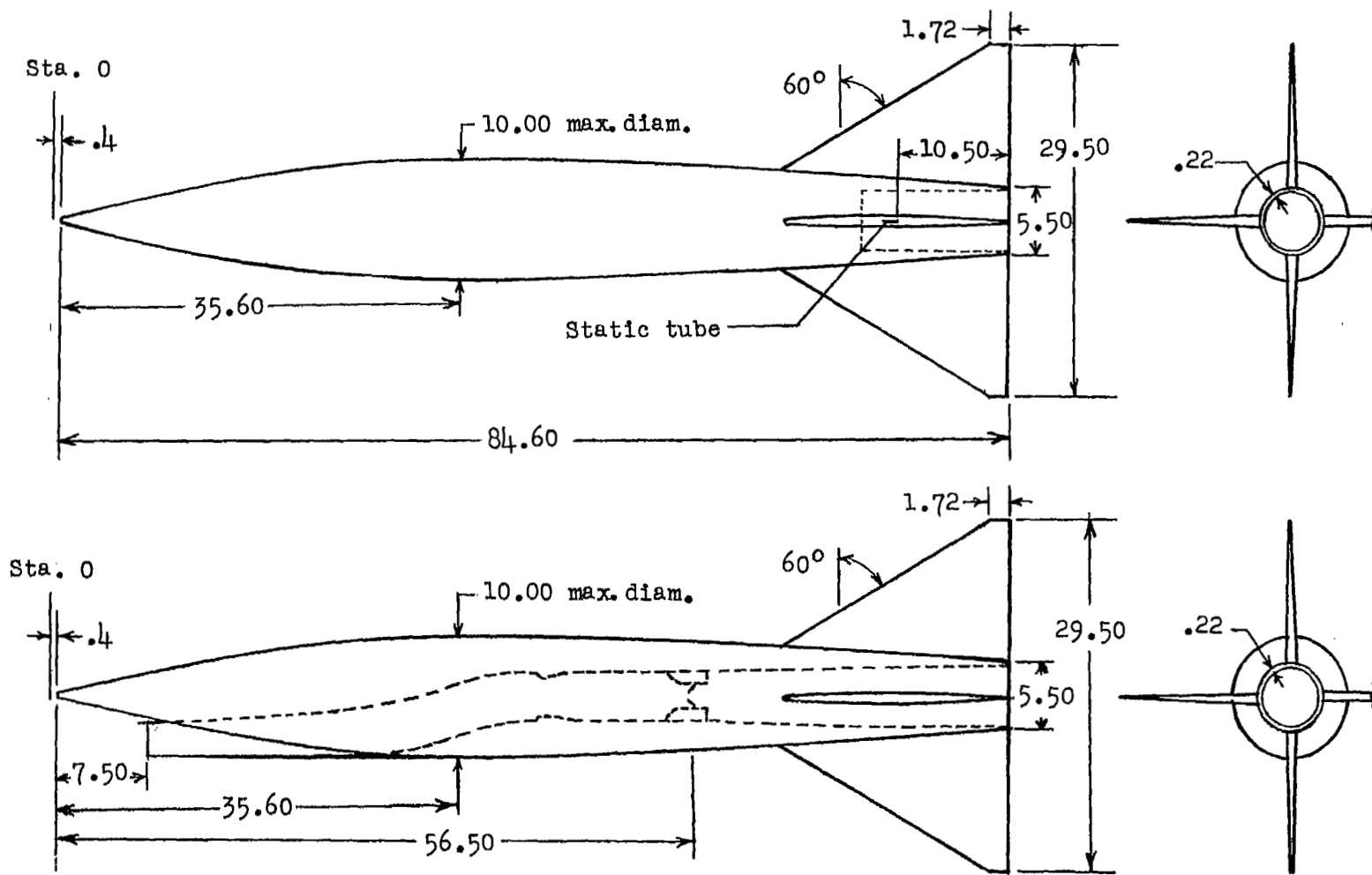


Figure 2.- General arrangement of the models. (All dimensions are in inches.)

Lip coordinates

x	y ₁	y ₂
0.018	0.021	0.017
.035	.032	.022
.070	.047	.027
.105	.054	.031
.140	.054	.033
.280	.054	.037
.560	.054	.037

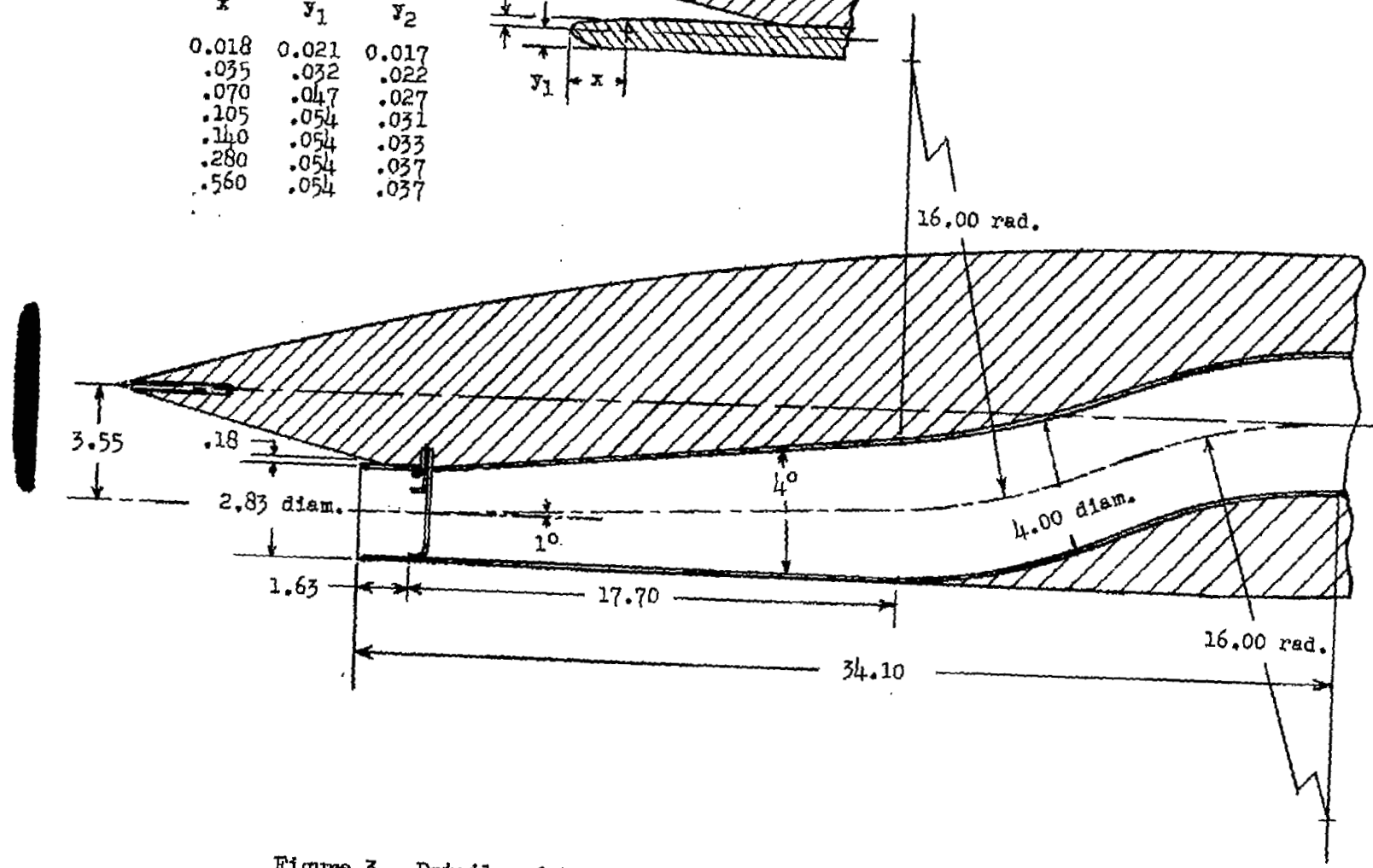
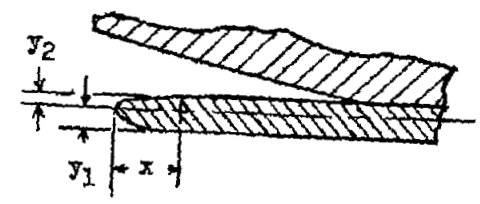


Figure 3.- Details of the inlet. (All dimensions are in inches.)

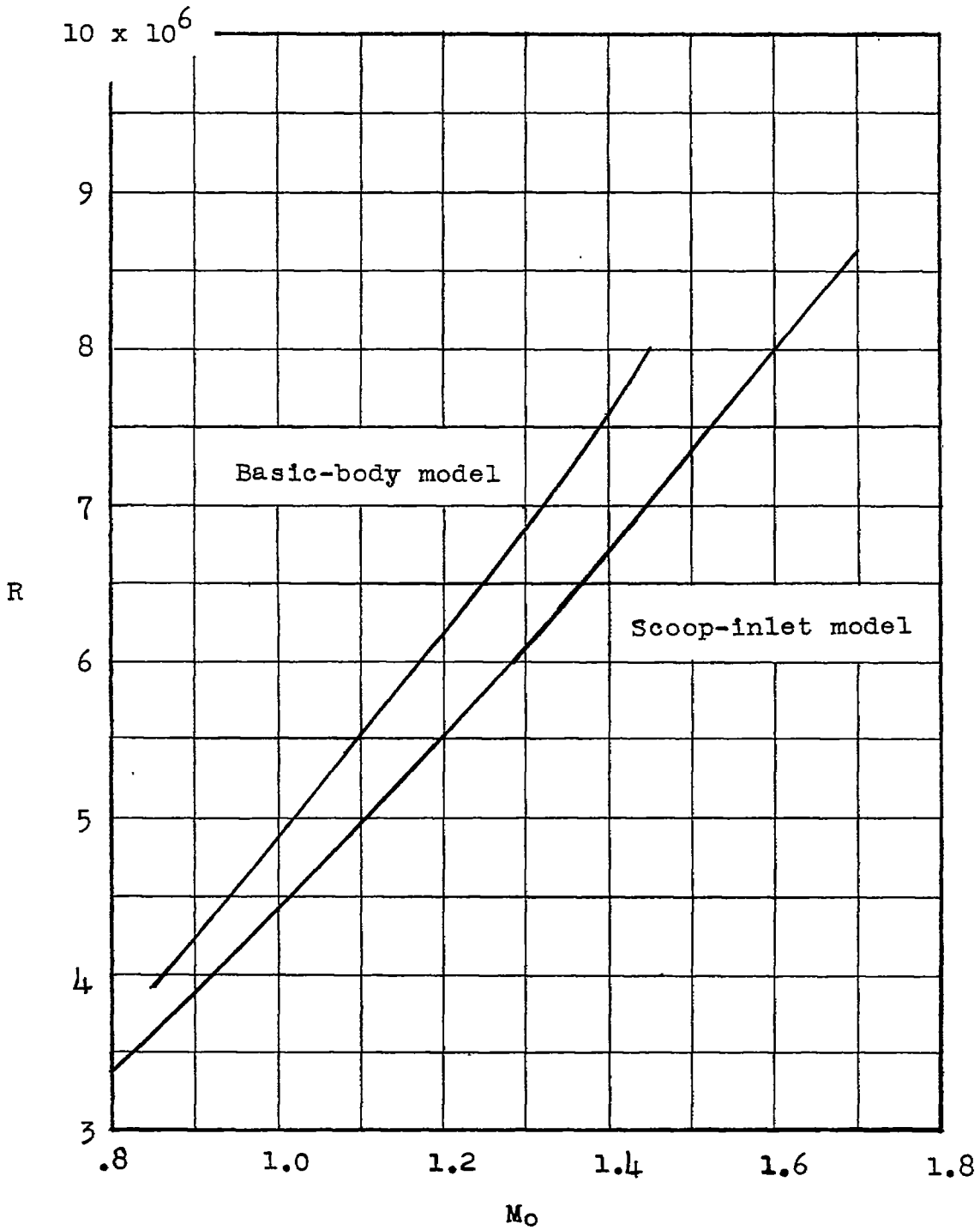


Figure 4.- Variation of Reynolds number based on body diameter with Mach number.

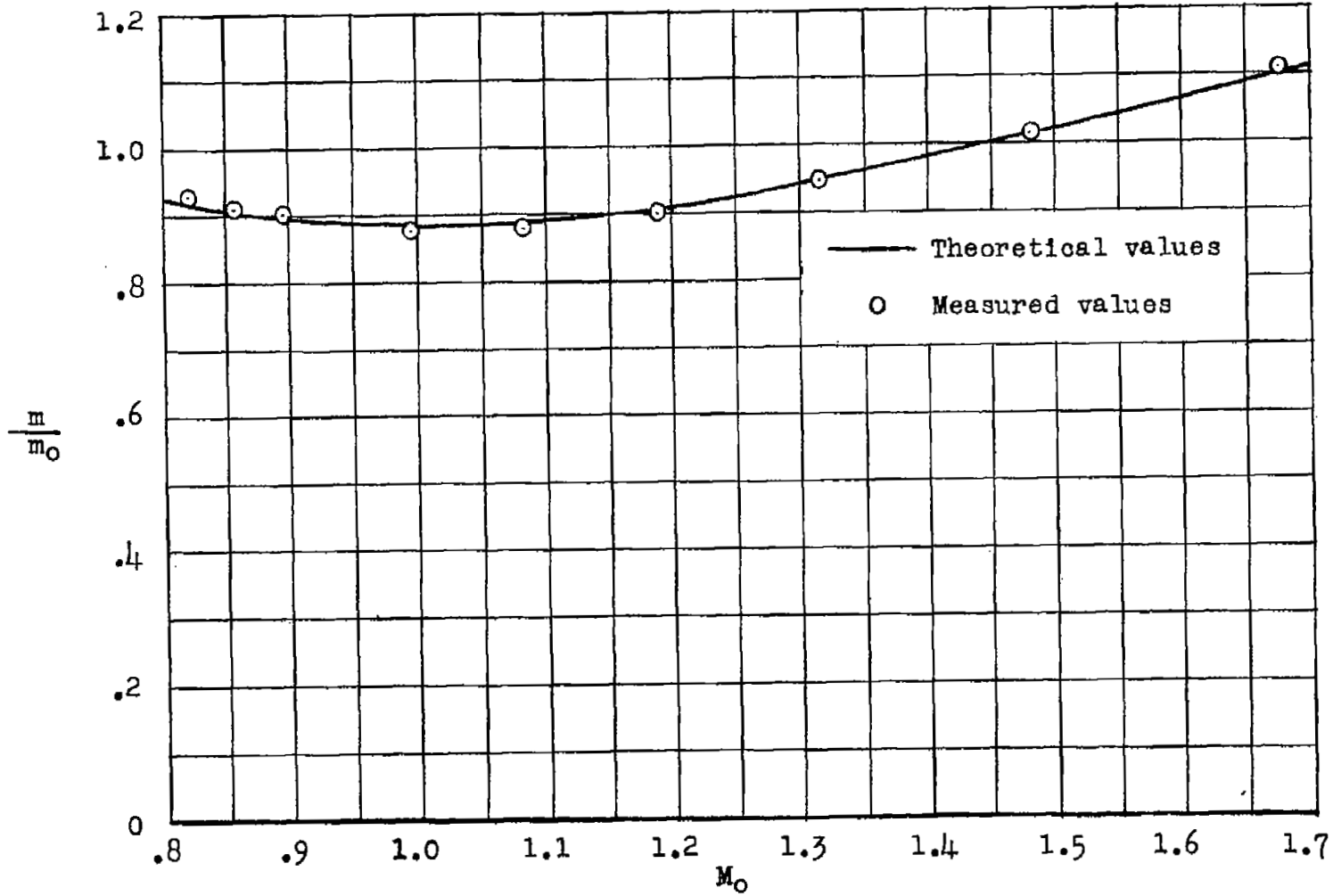


Figure 5.- Comparison of theoretical and measured values of maximum mass-flow ratio.

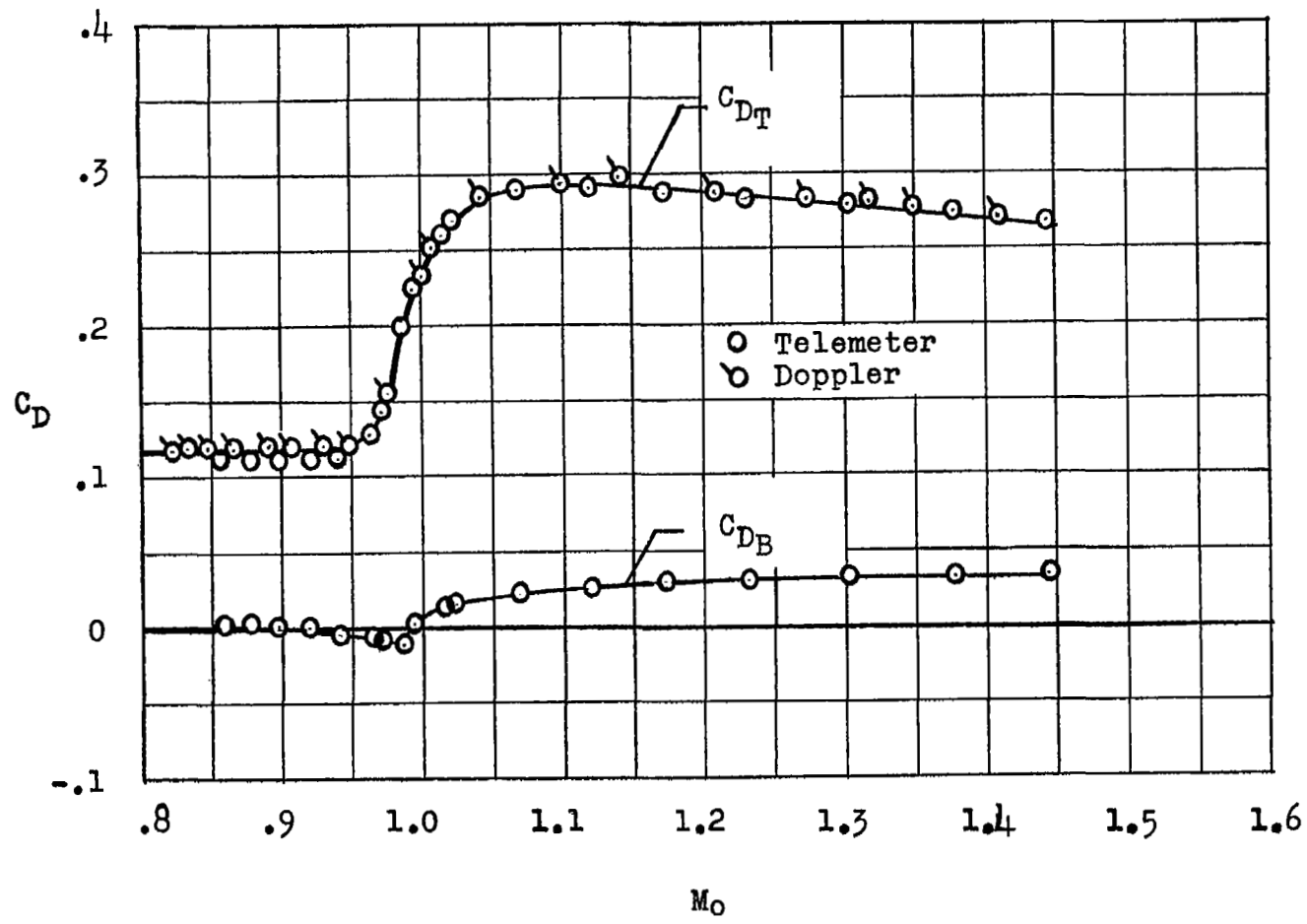


Figure 6.- Total and base drag coefficients as a function of Mach number for the parabolic-body model.

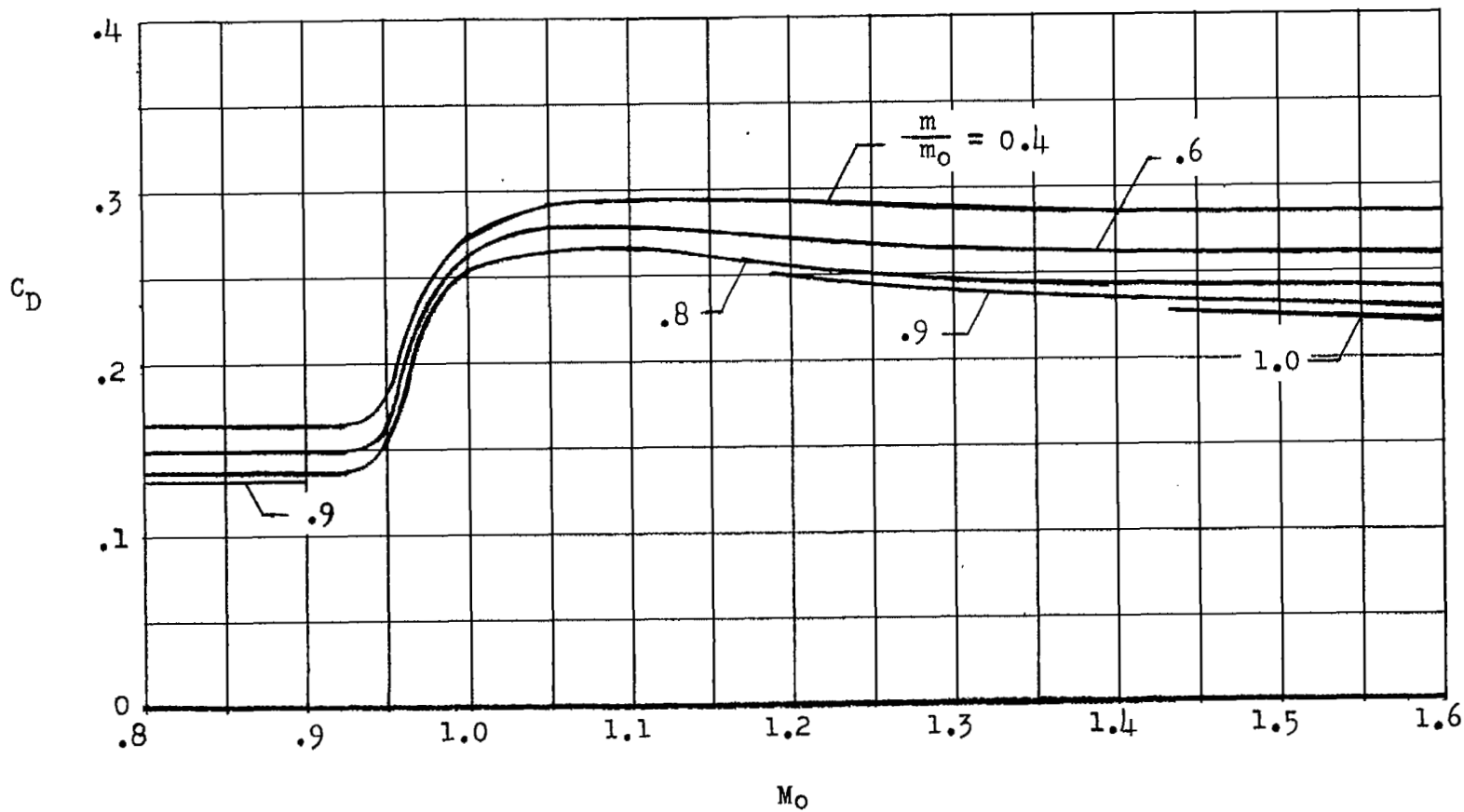


Figure 7.- Variation of external-drag coefficient of the scoop-inlet model with Mach number for several mass-flow ratios.

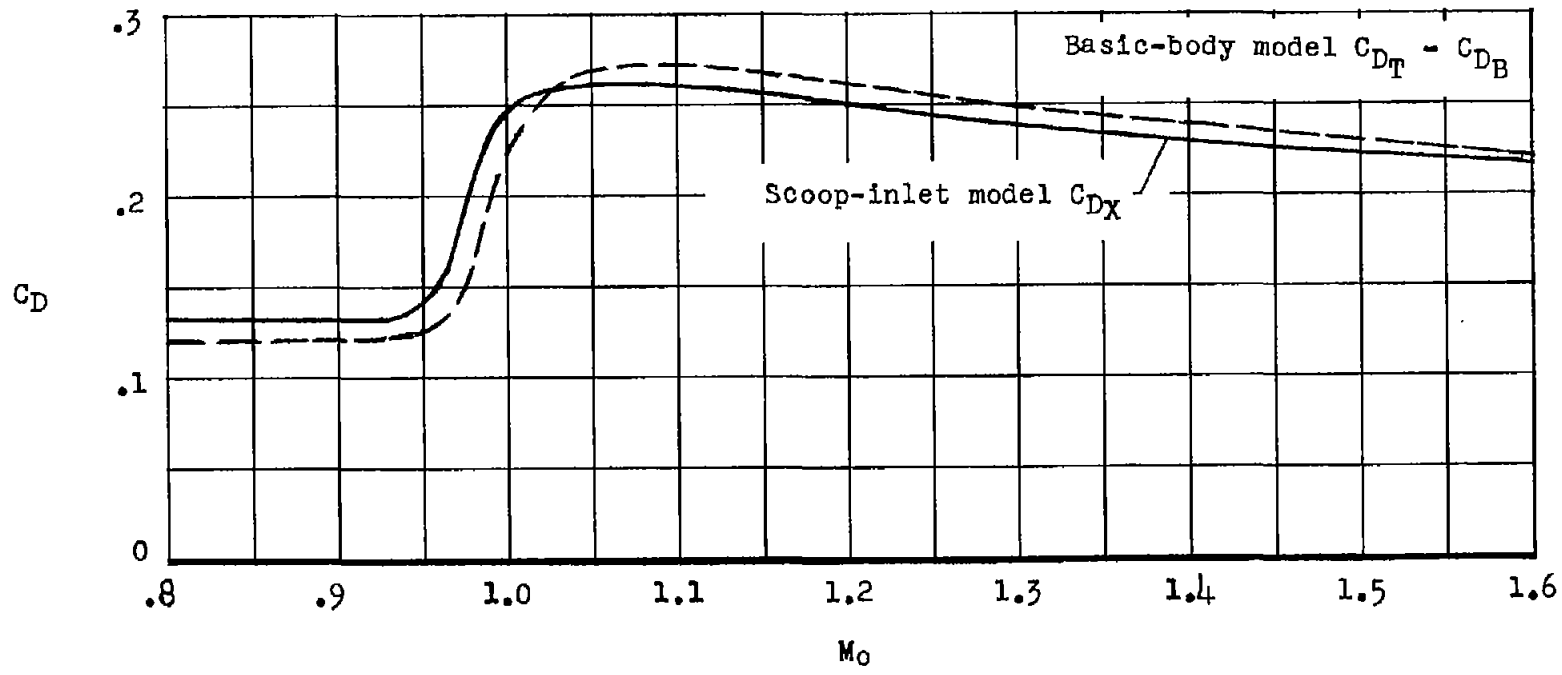


Figure 8.- Comparison of the external-drag coefficient of the scoop-inlet model at maximum mass-flow ratio with the total-minus-base drag coefficient of the parabolic body.

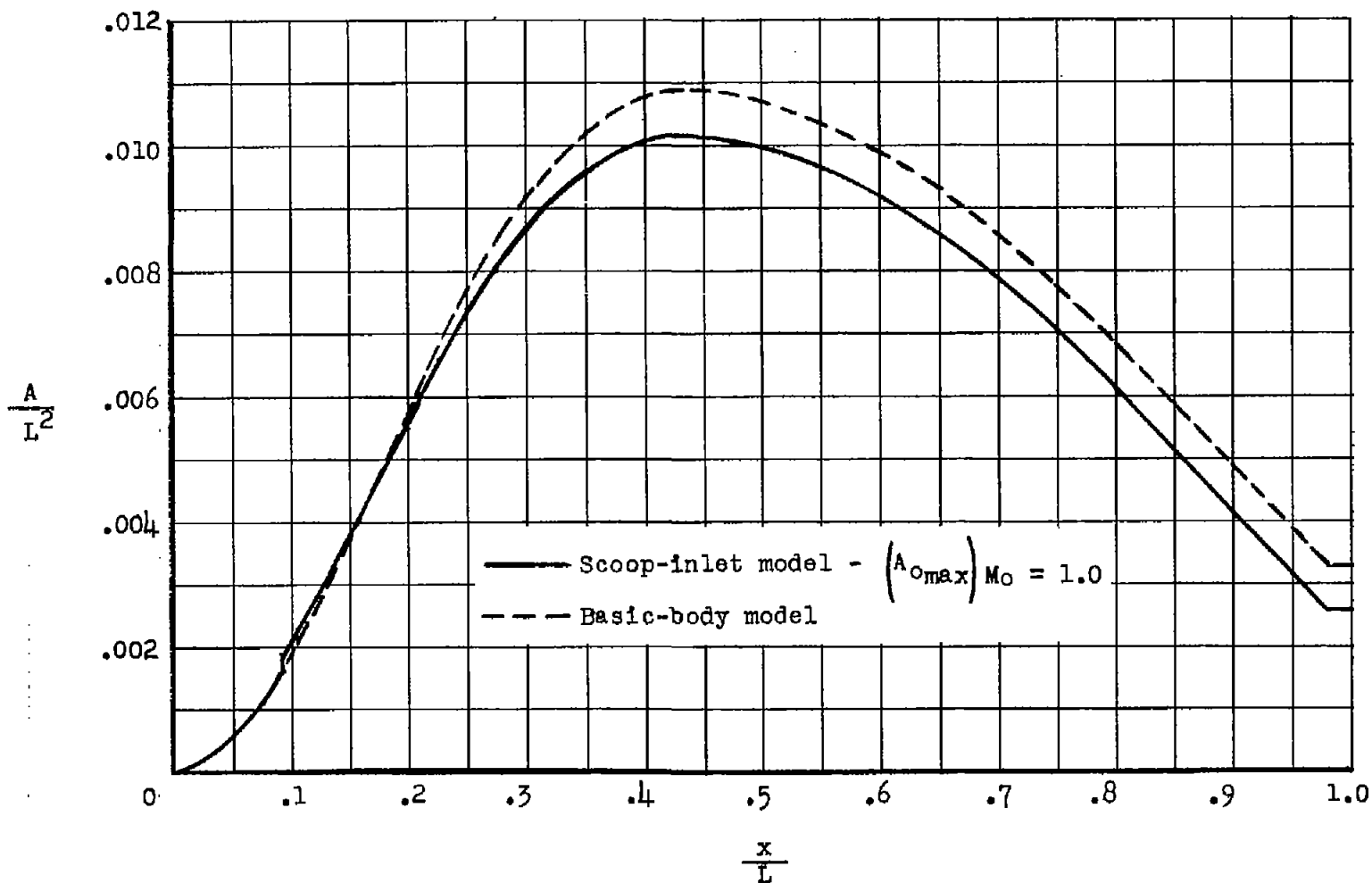


Figure 9.- The comparison of the longitudinal cross-sectional-area distribution of the basic-body model and the effective area distribution of the scoop-inlet model. (Fins have been omitted.)

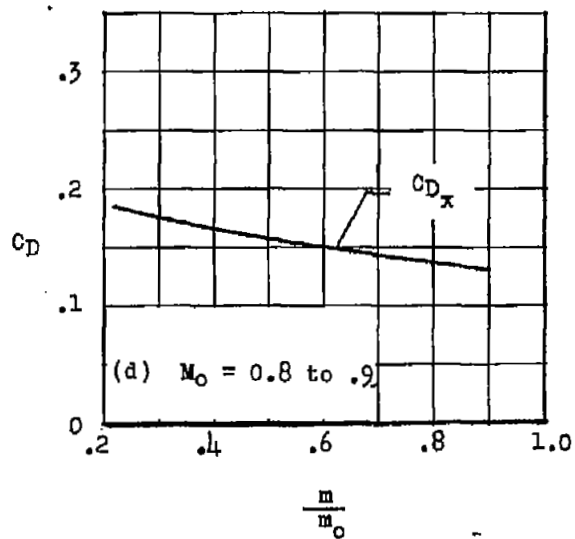
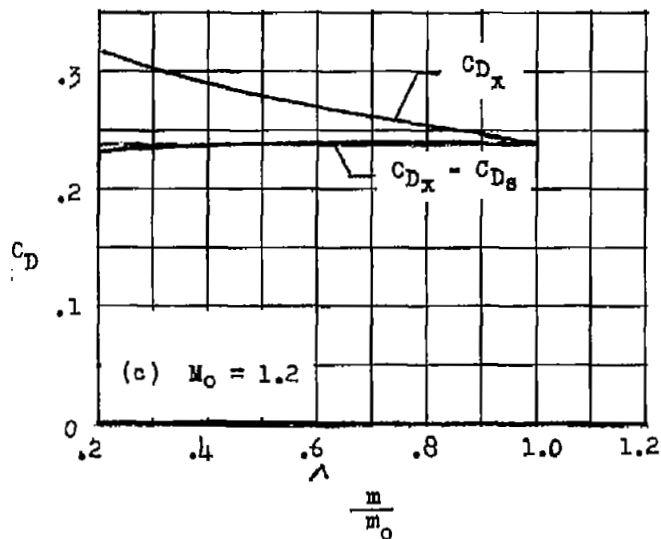
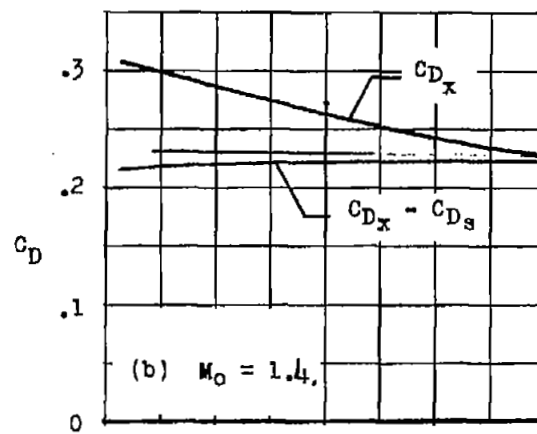
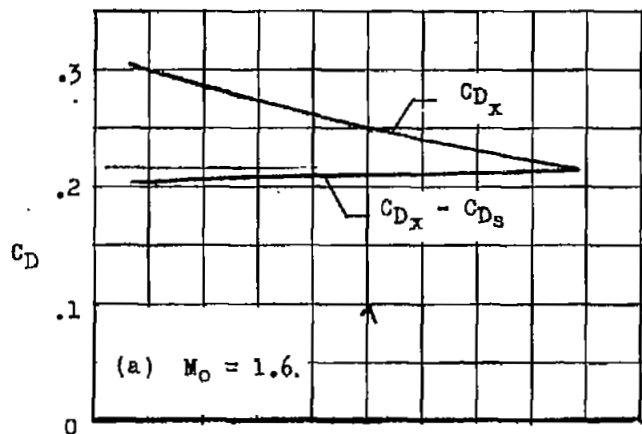


Figure 10.- Variation of external-drag coefficient with mass-flow ratio at several Mach numbers.

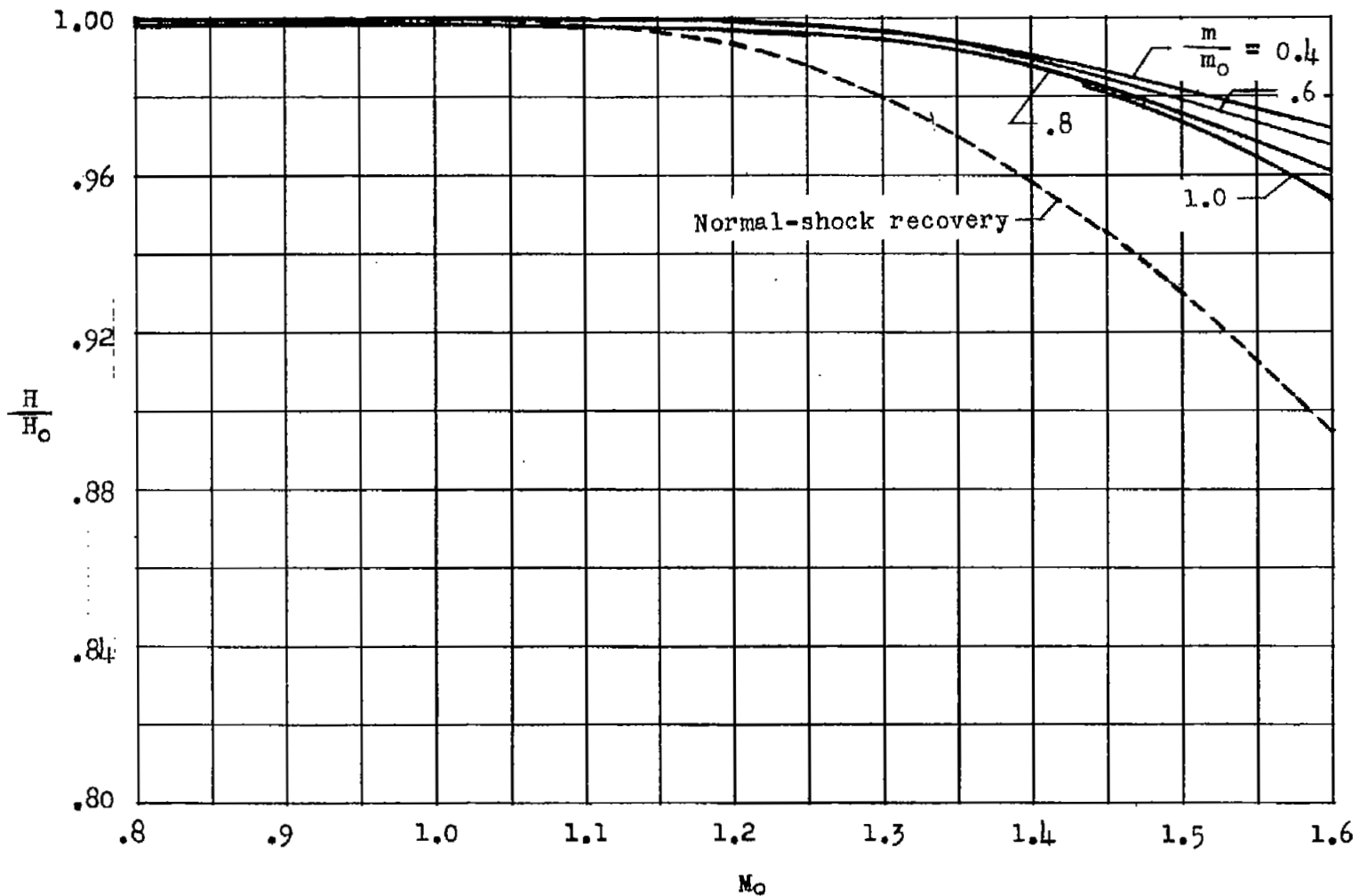


Figure 11.- Total-pressure recovery at the inlet-minimum-area station as a function of Mach number for several mass-flow ratios.

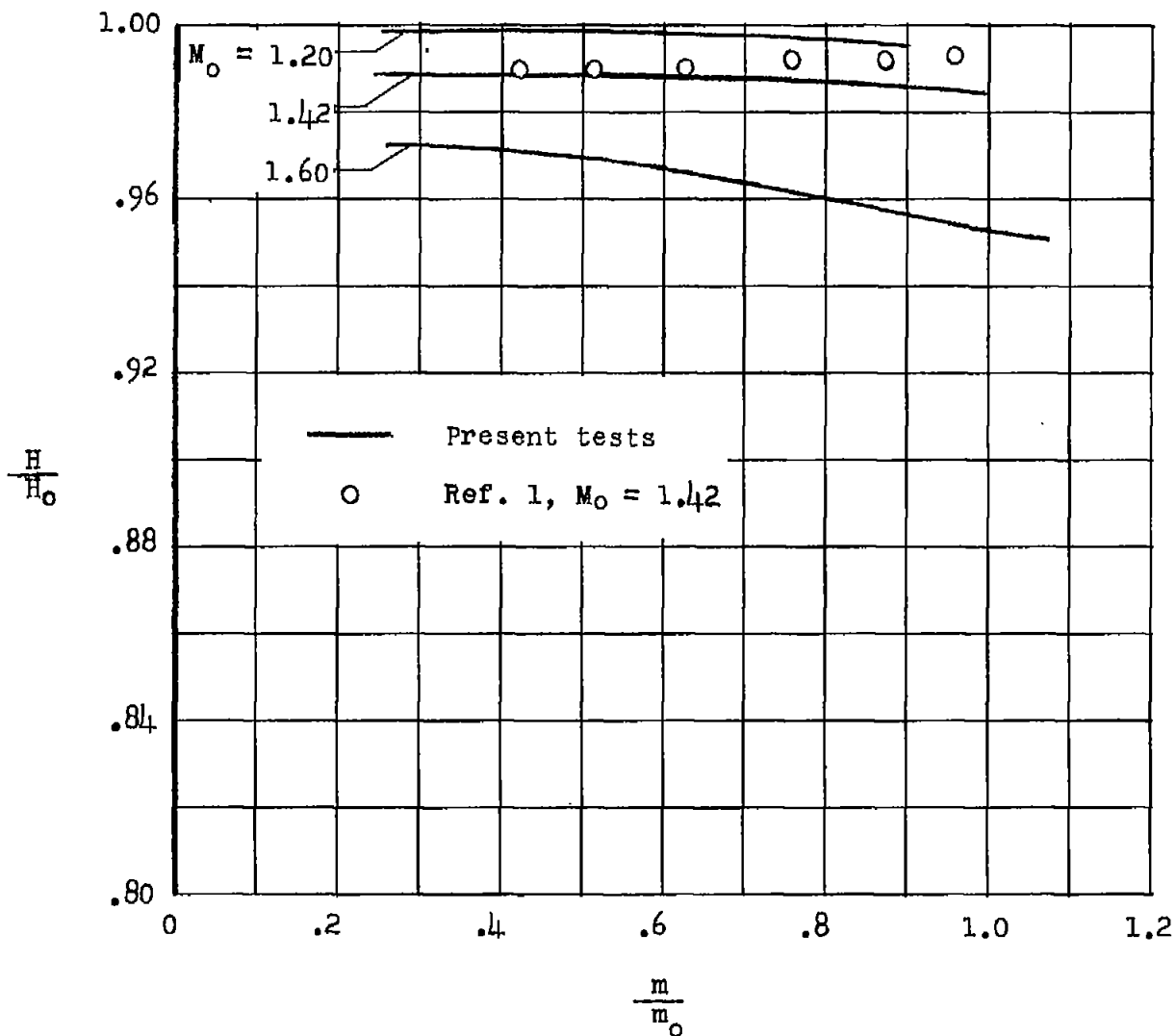
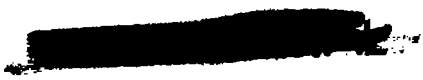


Figure 12.- Total-pressure recovery at the inlet-minimum-area station as a function of mass-flow ratio for several Mach numbers.



NASA Technical Library



3 1176 01437 1372

6
1

1
1

Figure 1

1
1

